EUKARYOTIC CELL, Feb. 2003, p. 181–190 Vol. 2, No. 1
1535-9778/03/$08.00+0 DOI: 10.1128/EC.2.1.181–190.2003
Copyright © 2003, American Society for Microbiology. All Rights Reserved.

TOK Homologue in *Neurospora crassa*: First Cloning and Functional Characterization of an Ion Channel in a Filamentous Fungus

Stephen K. Roberts*

Biology Department, Institute of Environment and Natural Sciences, Lancaster University, Lancaster LA1 4YQ, United Kingdom

Received 15 July 2002/Accepted 22 October 2002

In contrast to animal and plant cells, very little is known of ion channel function in fungal physiology. The life cycle of most fungi depends on the "filamentous" polarized growth of hyphal cells; however, no ion channels have been cloned from filamentous fungi and comparatively few preliminary recordings of ion channel activity have been made. In an attempt to gain an insight into the role of ion channels in fungal hyphal physiology, a homolog of the yeast K^+ channel (ScTOK1) was cloned from the filamentous fungus, *Neurospora crassa*. The patch clamp technique was used to investigate the biophysical properties of the *N. crassa* K^+ channel (NcTOKA) after heterologous expression of NcTOKA in yeast. NcTOKA mediated mainly time-dependent outward whole-cell currents, and the reversal potential of these currents indicated that it conducted K^+ efflux. NcTOKA channel gating was sensitive to extracellular K^+ such that channel activation was dependent on the reversal potential for K^+. However, expression of NcTOKA was able to overcome the K^+ auxotrophy of a yeast mutant missing the K^+ uptake transporters TRK1 and TRK2, suggesting that NcTOKA also mediated K^+ influx. Consistent with this, close inspection of NcTOKA-mediated currents revealed small inward K^+ currents at potentials negative of E_K. NcTOKA single-channel activity was characterized by rapid flickering between the open and closed states with a unitary conductance of 16 pS. NcTOKA was effectively blocked by extracellular Ca^{2+}, verapamil, quinine, and TEA^+ but was insensitive to Cs^+, 4-aminopyridine, and glibenclamide. The physiological significance of NcTOKA is discussed in the context of its biophysical properties.

The molecular identity and electrophysiological and structural properties of plasma membrane ion channels are well characterized in animal cells and increasingly so in plants (1, 2, 16). As a result, ion channels in these cells have been shown to be central to many aspects of cell biology, including elevation of cytoplasmic calcium during cell signaling, secretion, membrane potential control, nutrient uptake, and sensory perception. As a result of their biophysical characterization and molecular cloning, ion channels can be sorted into distinct families. The superfamily of K^+ channels is probably the most thoroughly studied. With reference to the animal literature, the voltage-gated K^+ channels (Shaker family) are outward rectifiers composed of four subunits, each subunit having the structural motif of S_{1-5}-P-S_6, where the "S" refers to the transmembrane spans (TMS) and the "P" is the pore-forming domain containing the conserved TXGYGD amino acid motif that forms the K^+ filter in the tetramer. Also characteristic of the Shaker-type channels is the presence of a voltage sensor in S_4 which is composed of positively charged residues at every third or fourth residue and moves with changes in membrane potential to trigger channel opening. Inwardly rectifying K^+ channels are similar to the Shaker-type channels except that each subunit of the tetramer contains only two TMS arranged as S_1-P-S_2 and they do not possess a voltage sensor (16). A new family of K^+ channels has recently been discovered which possess two pore-forming domains in each subunit and are likely to form dimers (10). The first example of a two-P-domain channel, TOK1 (also known as DUK1 or YORK), was identified in *Saccharomyces cerevisiae* and shown to possess eight predicted TMS (arranged as S_{1-5}-P_1-S_{6-7}-P_2-S_8) and to encode a non-voltage-gated outward rectifier (i.e., the absence of a voltage sensor in the TMS). Since the discovery of ScTOK1, many two-P-domain channels have been characterized from animal cells, all of which have four TMS arranged as S_1-P_1-S_{2-3}-P_2-S_4 and encode voltage independent inward rectifiers or open channels. They are proposed to function as highly regulated K^+-selective leak channels involved in the membrane potential control of nerve and muscle cells.

In contrast to animal and plant cells, little is known of ion channel function in fungi. To date, only two channels have been cloned from *S. cerevisiae* and characterized by using electrophysiological techniques. The plasma membrane channel, ScTOK1 (17, 18, 41), was first recorded by Gustin et al. (12) and has more recently been extensively studied with respect to its gating properties (e.g., see reference 22). Also, the vacuolar cation channel, YCV1 (3), has recently been identified as a TRP homolog in yeast (27). However, it is noteworthy that studies using the patch clamp technique (PCT) have identified other channel types in yeasts (5, 13, 31, 39). Unlike *S. cerevisiae*, most fungi are filamentous and polarized growth of hyphal cells is essential to their life cycle. However, no ion channels have been cloned from a filamentous fungus. Furthermore, there have been relatively few reports of ion channel activity from hyphal cells, the main reason being that the PCT, which is required for the rigorous study of ion channels, had been notoriously difficult to apply to their membranes, particularly the plasma membrane (20, 21; see also the review by Garrill and Davies [8]). For the detailed analysis of ion channel properties (i.e., selectivity and gating), the PCT demands for-

* Mailing address: IENS, Biology Department, Lancaster University, Lancaster LA1 4YQ, United Kingdom. Phone: 01524-593145. Fax: 01524-843854. E-mail: s.k.roberts@lancaster.ac.uk.

mation of a high resistance seal between the membrane and the patch clamp pipette (14). However, in most studies on hyphal plasma membrane, only suboptimal pipette-membrane seals were obtained by using protoplasts, which were derived by removing the fungal cell wall by using cell wall-degrading enzymes. Although the "sub-gigaohm seals" have been useful in mapping ion channel locations along fungal hypha (21), an extensive examination of the fundamental properties of ion channels (such as permeability and gating) has not been possible in these studies. The exception to this is a report of giga-ohm seals on enzyme-derived germling protoplasts from *Uromyces* (40). Recently, a laser ablation technique (originally developed for use on plant cells [36]) was used to remove the cell wall from fungal hyphae, and the exposed plasma membrane was found to be amenable to the PCT. This allowed, for the first time, a more rigorous identification of several types of plasma membrane ion channel from filamentous fungi. In *Aspergillus* spp., Roberts et al. (30) identified anion efflux and a K^+ efflux channel (unpublished data) whereas Véry and Davies (38) identified K^+ and Ca^{2+} uptake channels in *Neurospora crassa*. However, despite the successes achieved with the laser ablation PCT on filamentous fungi, progress has been slow.

In the present study an alternative approach to the laser-assisted PCT was used to investigate ion channel function in filamentous fungi. Specifically, gene cloning and heterologous expression techniques were used to functionally characterize a K^+ channel from *N. crassa* (NcTOKA). Structural analysis revealed that *NcTOKA* encoded an eight-TMS, two-P-domain-type K^+ channel. Yeast cells expressing NcTOKA exhibited outwardly rectifying K^+-permeable currents that were not present in nontransformed yeast cells. The present study represents the first reported molecular identification and characterization of an ion channel from a filamentous fungus.

MATERIALS AND METHODS

Strains and growth media. The *N. crassa* strain used was RL21a, which was obtained from the Fungal Genetic Stock Center (FGSC 2219). Conidia were inoculated in YPD medium (1% yeast extract, 2% peptone, 2% glucose) and incubated for 14 to 16 h at 30°C shaking at 150 rpm. A *trk1Δ trk2Δ tok1Δ* triple deletion strain of *S. cerevisiae* (*WΔ3TOK1Δ*; *MAT***a** *ura3 his3 trp1 ade2 trk1Δ::LEU2 trk2Δ::HIS3 tok1Δ::TRP1*) was used and has been described elsewhere (31). Unless otherwise stated, *WΔ3TOK1Δ* cells were grown overnight at 30°C with shaking at 100 rpm in 30 ml of liquid media (yeast nitrogen broth [Difco Laboratories], 100 mM KCl) containing either 2% (wt/vol) glucose or galactose and supplemented with adenine.

RNA isolation. Fungal colonies were fixed in liquid nitrogen, and total RNA isolation was performed with the RNeasy Plant Mini Kit (Qiagen) from ca. 100 mg of frozen mycelia. According to manufacturer's recommendations, a buffer containing guanidium hydrochloride was used instead of a buffer containing guanidium isothiocynate to avoid solidification of the samples due to secondary metabolites in mycelia of fungi. An average yield of ca. 1 μg of total RNA per mg of frozen mycelium was isolated. Approximately 100 μg of total RNA was treated with 15 U of RNase free DNase I (Gibco) according to manufacturer's recommendations. mRNA was isolated from DNase-treated RNA by using a Mini mRNA extraction kit (Qiagen).

cDNA synthesis and isolation of full-length NcTOKA cDNA. cDNA was prepared from 100 ng of mRNA isolated from *N. crassa* (grown for 16 h in YPD) by using the SMART RACE cDNA amplification kit (Clontech). The DNA sequence from the genomic DNA database from the Whitehead Institute *Neurospora* Sequencing Project (assembly version 1; http://www-genome.wi.mit.edu) was used to design gene specific primers A1 (5′ RACE primer [TACCGTGGG ATTTGGCGATTACTACC]) and A2 (3′ RACE primer [CCACTCGCCTCTT ATGACTCTCTTCG]). Primers A1 and A2 were used to perform 5′ and 3′ RACE reactions according to manufacturer's recommendations. PCR was performed by using the Advantage2 cDNA PCR system (Clontech). PCR products were subcloned into pGEMT-Easy vector (Promega) and sequenced. To generate the full-length NcTOKA cDNA, primers were designed from the 5′ end of the RACE product sequence and the 3′ end of the 3′ RACE product sequence. PCR was performed by using high-fidelity *Pfu* turbo polymerase (Stratagene) and primers A3 (5′-TTAATACTACCTATCTGACAACATGCAGGACGCTGG) and A4 (3′-TTACAGACCAGGCATGAAGGTGTCCGTTTGC). The full-length NcTOKA clone was "A-tailed" according to the manufacturer's recommendations and subcloned into the PCR2.1-TOPO vector (Invitrogen). NcTOKA was excised from PCR2.1-TOPO vector by using *Eco*RI restriction enzyme and subcloned into *Eco*RI-linearized vector pYES2 (Clontech). NcTOKA was sequenced, and the resulting plasmid was called pYES2-NcTOKA. NcTOKA was submitted to the European Molecular Biology Laboratory (EMBL) database on 10 March 2002 and was assigned accession number AJ510245.

The yeast strain, *WΔ3TOK1Δ*, was transformed with pYES2-NcTOKA as previously described (9).

Spheroplast isolation. A method based on that described by Bertl and Slayman (3) was used for spheroplast isolation. Cells were harvested from 10 ml of suspension culture by centrifugation (188 × *g* for 5 min). The cell pellet was resuspended in 10 ml of buffer A (50 mM KH_2PO_4–40 mM 2-mercaptoethanol adjusted to pH 7.0 with KOH), pelleted again, resuspended in 2 ml of buffer B (1.2 M sorbitol, 50 mM KH_2PO_4, 40 mM 2-mercaptoethanol, 10 mg of zymolyase 20T [ICN]/ml, and 2,000 U of β-glucuronidase [Sigma]/ml adjusted to pH 7.0 with KOH) and incubated at 30°C, with shaking at 100 rpm. After 90 min, the digest was centrifuged at 188 × *g* for 5 min, and the pellet was resuspended in 5 ml of ice-cold buffer C (1 M sorbitol, 10 mM HEPES, and 1 mM $CaCl_2$ adjusted to pH 7.0 with KOH) and centrifuged at 188 × *g* for 5 min. The pellet was resuspended in 1 ml of buffer C and stored on ice. Spheroplasts with diameters of 4 to 5 μm were used.

Electrophysiology. All recordings were made in a continuously perfused chamber in which a glass coverslip formed the base to which the spheroplasts adhered loosely. Patch pipettes were fabricated on a two-stage puller (Kopf Instruments, Tujunga, Calif.) from borosilicate glass (Kimax-51; Kimax Products, Vineland, N.J.). To reduce pipette capacitance, electrodes were coated by dipping the pipette tip into a 50% (wt/wt) mixture of mineral oil and Parafilm (American National Can., Chicago, Ill.). Positive pressure was maintained at the tip to prevent its blocking. Pipette resistances varied between 5 to 10 MΩ. An Ag/AgCl reference electrode was connected to the bath chamber via a 3 M KCl agar bridge. Whole-cell currents were recorded at room temperature (ca. 20°C) with an RK-400 amplifier (Biologique, Claix, France) connected to an A/D converter (Digidata 1200; Axon Instruments, Foster City, Calif.). Recording and storage of data were controlled by the software package pClamp 8.01 (Axon Instruments) and a personal computer. Liquid junction potential was measured and corrected for as described by Neher (26). Tip potentials were recorded and found to be negligible (<2 mV). Whole-cell data were filtered at 3 kHz. Single-channel data were sampled at 5 kHz and filtered at 1 kHz.

Solutions used in electrophysiology. All solutions were filtered (0.2-μm pore diameter; Millipore) before use and were adjusted to 700 mOsmol kg^{-1} with sorbitol. Seals in excess of 12 GΩ were formed in sealing solution that contained 10 mM KCl, 10 mM $CaCl_2$, 5 mM $MgCl_2$, and 5 mM HEPES-Tris base (pH 7.4). After we obtained the whole-cell configuration (indicated by an increase in capacitance of between 0.5 to 0.7 pF), the solution was replaced by a standard bath solution (SBS; 1 mM $CaCl_2$, 10 mM HEPES-Tris base; pH 7.0) containing various concentrations of KCl unless otherwise stated. The small size of the sphereoplast and the coating of the pipette to the tip with an oil-parafilm mixture resulted in the dramatic reduction of pipette capacitance that allowed effective compensation by the amplifier. Unless otherwise stated, pipettes were filled with 10 mM KCl, 100 mM potassium gluconate, 5 mM $MgCl_2$, 4 mM magnesium ATP, 10 mM HEPES, 4 mM EGTA, and 20 mM KOH (pH 7.4). Ionic equilibrium potentials were calculated after correction for ionic activity by using GEOCHEM-PC (28).

RESULTS

Structural analysis of NcTOKA. A search of the *Neurospora* Sequencing Project Database (see Materials and Methods) for peptide sequences homologous to the pore domain from several K^+ channel proteins led to the identification of a genomic DNA sequence which, after translation, displayed the presence

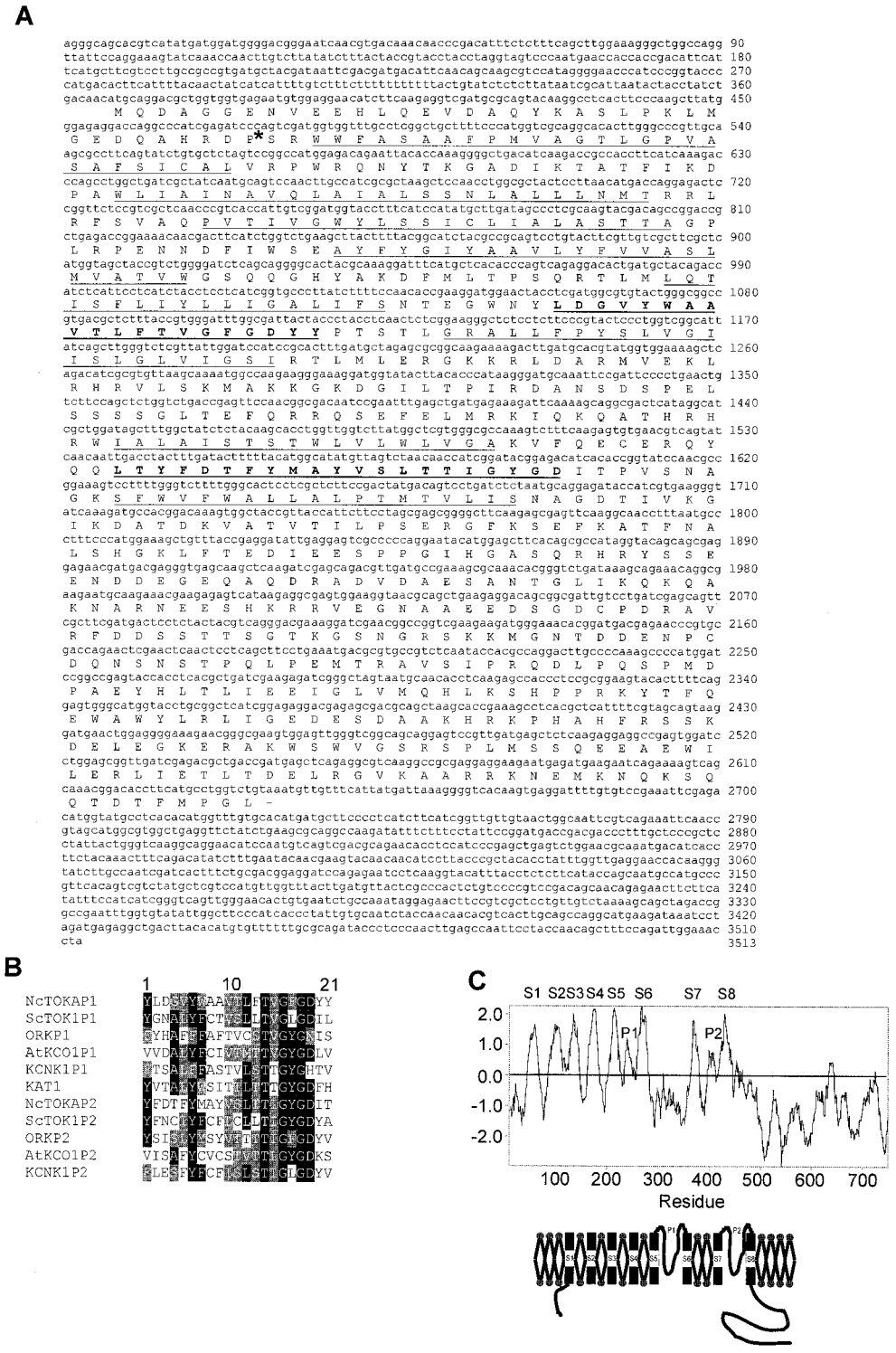

FIG. 1. Structural properties of NcTOKA. (A) Nucleotide sequence of the full-length NcTOKA, along with the amino acid sequence of the longest open reading frame. Transmembrane segments are underlined, and P domains are bold and underlined. The asterisk represents the position of a 75-bp intron identified from the genomic DNA sequence. (B) Alignment of the P domains of NcTOKA and other K^+ channels. Identical and similar residues are boxed in black and gray, respectively. The accession numbers are as follows: ScTOK1, P40310; ORK1, Q94526; AtKCO1, CAA65988; KCNK1, U76996; and KAT1, S32816. (C) Hydropathy profile and deduced topology for NcTOKA. Hydrophobicity values were calculated according to the method of Kyte and Doolittle (17a; unpublished data) (window size of 17 residues) and are plotted against amino acid position. The TMS and P domains are labeled.

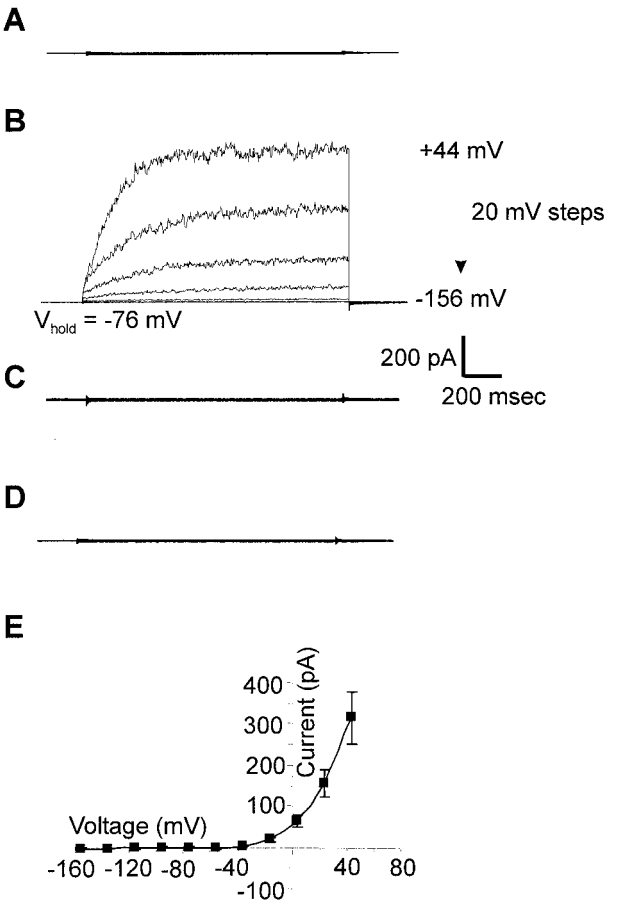

FIG. 2. NcTOKA whole-cell currents. SBS containing 10 mM KCl and 10 mM $CaCl_2$ was used. (A) Whole-cell current traces in *WΔ3TOK1Δ* yeast cells in response to voltage pulses ranging from +44 mV to −156 mV in 20-mV steps. Holding voltage was −76 mV. (B) Whole-cell current traces from *WΔ3TOK1Δ* yeast cells transformed with pYES2-NcTOKA plasmid and cultured on galactose-containing medium. Voltage pulses as for panel A. (C) Same as panel B except that cells were cultured on glucose-containing media. (D) Whole-cell current traces from *WΔ3TOK1Δ* cells transformed with pYES2 plasmid and cultured on galactose-containing medium. (E) Mean current voltage-relationship of *WΔ3TOK1Δ* yeast expressing NcTOKA (n = 18; error bars denote ± the SEM).

of two pore-like domains in the same open reading frame (contig 1.146). Primers designed from the genomic DNA sequence were used in RACE PCR experiments to identify the full-length cDNA which encoded the amino acid sequence shown in Fig. 1A. Comparison of genomic DNA and cDNA sequences revealed that they were identical except for a 75-bp intron in the genomic DNA sequence 111 bp downstream of the initial ATG codon (Fig. 1A). The size of the intron is typical for filamentous fungi. The nucleotide sequences of GTAAGT and AG bordered the 5′ and 3′ termini of the intron, respectively, and have been found to be conserved in filamentous fungal introns (11).

The longest open reading frame encoded a 757-amino-acid protein that shared highest homology to the yeast K^+ channel, ScTOK1 (23% identity, 41% similarity), but did not show significant sequence conservation with other cloned K^+ channels except in the P domains (Fig. 1B). The hydropathy plot shown in Fig. 1C predicted eight hydrophobic transmembrane segments (S_1 to S_8) and two P domains, P_1 and P_2, flanked by TMS S_5 and S_6 and TMS S_7 and S_8, respectively. Furthermore, none of the TMS contained regularly spaced charged residues that have been shown to form the voltage sensor in voltage-gated Shaker-type K^+ channels. These characteristics identified the K^+ channel from *Neurospora* as a TOK1 homolog and consequently is referred to as NcTOKA.

Functional expression of NcTOKA channels. NcTOKA was subcloned into the yeast expression vector, pYES2, downstream of the GAL1 promoter and the pYES2-NcTOKA plasmid was transformed into the yeast triple mutant, *WΔ3TOK1Δ*. This mutant has the K^+ uptake (*trk1* and *trk2*) and K^+ efflux (*tok1*) transporters deleted (31). The biophysical properties of NcTOKA channel activity were investigated by using the PCT. Using SBS containing 10 mM K^+ and Ca^{2+}, no currents were observed in the untransformed *WΔ3TOK1Δ* (n = 9; Fig. 2A). However, the same yeast strain transformed with pYES2-NcTOKA and cultured in galactose-containing medium exhibited the large whole-cell currents shown in Fig. 2B. These large time-dependent outward currents were absent in (i) *WΔ3TOK1Δ* cells transformed with pYES2-NcTOKA and cultured in glucose-containing culture medium (n = 9; Fig. 2C) and in (ii) *WΔ3TOK1Δ* cells transformed with pYES2 (n = 8; Fig. 2D). Thus, these results demonstrated that the large, time-dependent, and depolarization-activated outward currents (314 ± 64 pA at +44 mV; n = 18; Fig. 2E) were the result of the functional expression of NcTOKA.

Biophysical properties. The NcTOKA-mediated currents were composed mainly of a time-dependent activating component that could be roughly fitted by an exponential function (Fig. 3A) with a time constant (τ) that increased as the voltage decreased from +44 to −36 mV (Fig. 3B). The outward current was also composed of a small instantaneous component. However, the ratio of instantaneous to time-dependent current was dependent on the holding potential (V_{hold}) prior to the activating depolarization pulse. Figure 3C shows a typical experiment in which the membrane potential was held at −76 mV (negative of the equilibrium potential for K^+) and then stepped to an activating depolarization voltage. Subsequent depolarization of the membrane induced the same magnitude of outward current but with a significant decrease in the ratio of instantaneous to time-dependent current. However, holding the membrane potential at more negative membrane potentials (i.e., −156 mV) abolishes the instantaneous component of the outward current during subsequent membrane depolarizations (Fig. 3C). A similar phenomenon has been reported for ScTOK1 currents and is proposed to represent channel activation proceeding through a series of closed transition states prior to entering the open state with increasing negative potentials "trapping" the channel in a deeper closed state (18, 37). Thus, the instantaneous currents might reflect the transition from a "shallow" closed state to the open state that is characterized by very rapid ("instantaneous") rate constants.

Selectivity. Deactivation "tail" currents could be resolved upon repolarizing the membrane to negative potentials when extracellular K^+ was 10 mM or more. These currents were apparent when viewed on an expanded current axis (see Fig. 4 and 5A) and after compensation of whole-cell and pipette

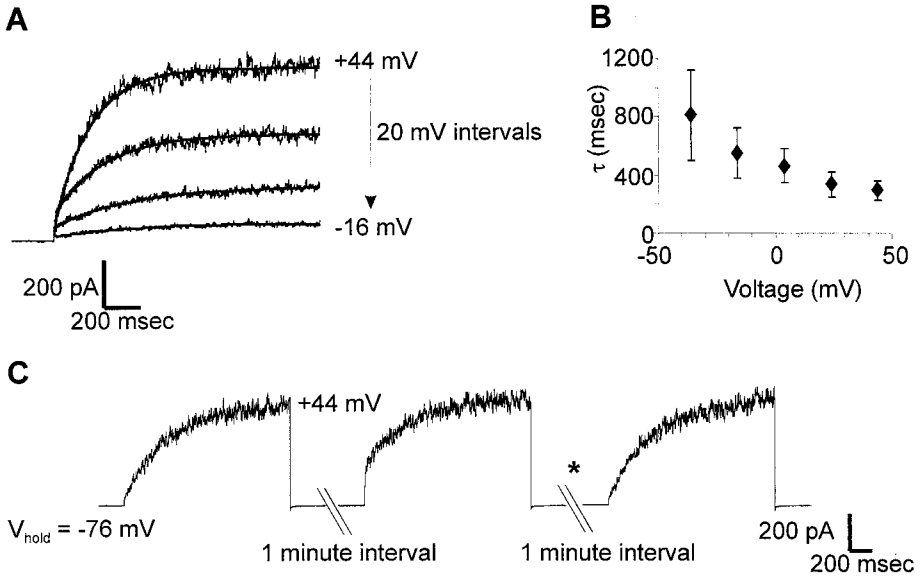

FIG. 3. Activation kinetics of NcTOKA whole-cell currents. Currents recorded with SBS containing 10 mM KCl and 10 mM $CaCl_2$. (A) Example of least-square fits of equation 1: $I = I_{ss} \exp(-t/\tau) + C$, where I_{ss} is the steady-state current and C is a constant offset. Currents result from voltage pulses ranging from +44 mV to −26 mV in 20-mV steps. The holding voltage was −76 mV. (B) Voltage dependence of the time constants (τ) of activation. Values are the mean (± the SEM) of six independent experiments. (C) Currents recorded from the same cell in response to voltage steps to +44 mV at 1-min intervals from a holding potential (V_{hold}) of −76 mV. The asterisk denotes the voltage step to −156 mV of 2-s duration ending 1 s prior to the voltage step to +44 mV.

capacitance (see Materials and Methods). Tail current protocols were used to determine the major ion responsible for the outward currents. Outward currents were activated by a depolarizing prepulse, followed by steps back to more negative potentials, giving rise to deactivation tail currents (Fig. 4). Reversal potentials (E_{rev}) were determined as described in the legend to Fig. 4. The mean (± the standard error of the mean [SEM]) reversal potential of the outward current in SBS containing 10 mM KCl was −53 ± 2.4 mV (n = 6). This was much closer to the reversal potential for K^+ (E_K = −62 mV) than for Cl^- (E_{Cl} = +13 mV). When the extracellular K^+ concentration was increased to 60 mM, E_{rev} followed the change in E_K (i.e., E_K = −19 mV; E_{rev} = −21 ± 2 mV [n = 4]), indicating K^+ efflux was mainly responsible for NcTOKA-mediated currents.

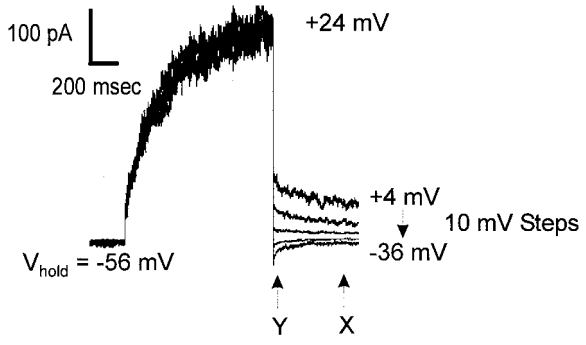

FIG. 4. Measurements of reversal potentials (E_{rev}) of NcTOKA whole-cell currents. Tail currents resulted from a voltage step to +24 mV, followed by steps back to pulses ranging from +4 mV to −36 mV in 10-mV steps. The holding voltage was −56 mV. SBS containing 60 mM KCl was used. The reversal potential of the tail current was determined by calculating the amplitude of the steady-state tail current (marked "X") and 50 ms after induction of the tail current (marked "Y"). Current amplitude values measured at point Y were subtracted from those at point X and plotted against voltage. The potential at which X − Y = 0 (i.e., E_{rev}) was determined from linear regression. Note that although capacitance currents were compensated for (see Materials and Methods), the current amplitude at Y was taken 50 ms after induction of the tail current so as to avoid contamination from any uncompensated capacitance currents.

NcTOKA inward currents. Two major K^+ uptake transporters, TRK1 and TRK2, enable wild-type yeast to grow in low-K^+-containing medium (submillimolar). However, *WΔ3TOK1Δ* is a *trk1Δ trk2Δ* mutant and thus is only able to survive on medium with a high K^+ content (>10 mM). Expression of NcTOKA was able to support growth of *WΔ3TOK1Δ* cells in medium containing <10 mM K^+ (Fig. 5A), indicating that NcTOKA was able to mediate K^+ uptake. Nontransformed *WΔ3TOK1Δ* cells exhibited the same growth phenotype as cells transformed with the empty vector, indicating that the phenotype was specific for NcTOKA expression. Consistent with NcTOKA mediating K^+ uptake, small inward currents could be observed at voltage negative of E_K in *WΔ3TOK1Δ* cells transformed with pYES2-NcTOKA (Fig. 5B). The reversal potentials of these inward currents followed shifts in E_K, indicating that they were carried by K^+ influx (Fig. 5C). It is noteworthy that the inward currents were only apparent when currents were viewed on an expanded scale.

Gating. The threshold potential for the activation of the outward current appeared to follow changes in extracellular K^+ (Fig. 5D). The sensitivity of NcTOKA channel gating to extracellular K^+ was examined by fitting a Boltzmann function to the relationship between the chord conductance of the outward current and voltage. In SBS containing 1, 10, and 60 mM

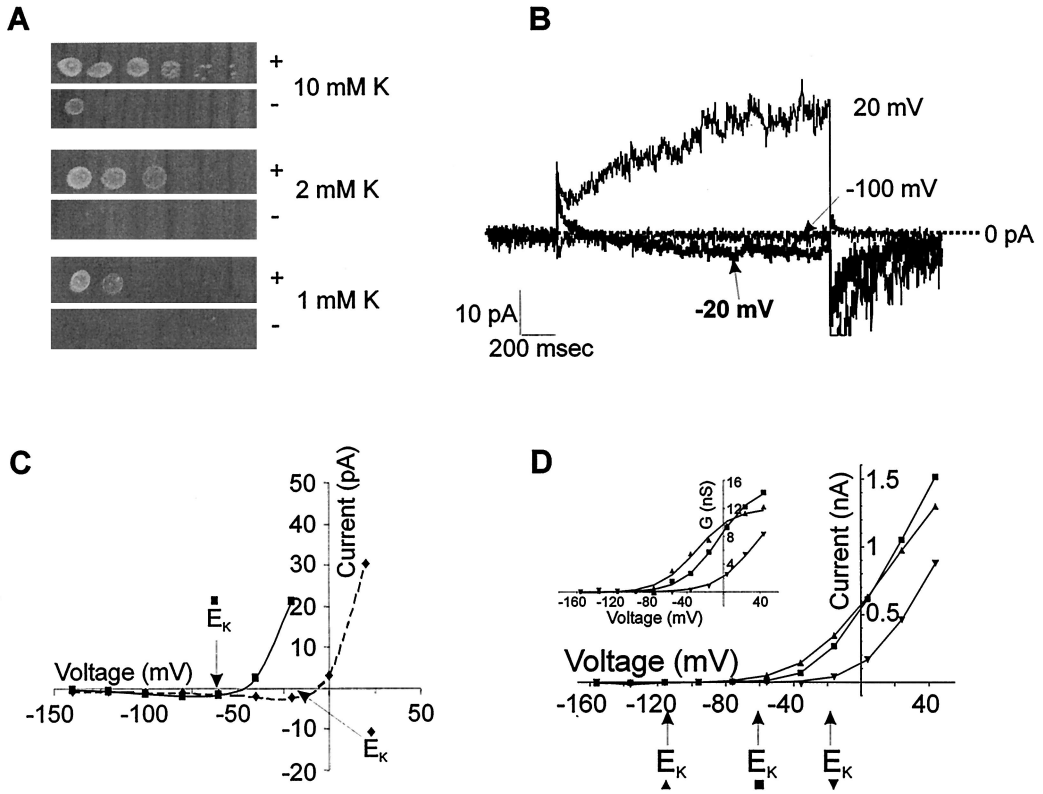

FIG. 5. (A) Expression of NcTOKA overcomes K^+-limited growth phenotype of the WΔ3TOK1Δ yeast mutant. The leftmost spots show patterns of growth after 3 days at 30°C after innoculation with 5 μl of culture at 0.5×10^8 cells/ml. Serial 10-fold dilutions of the first inocula are shown on the right. Growth is on arginine-phosphate medium (33) containing adenine and galactose and supplemented with 1, 2, or 10 mM KCl. "+" and "−" denote WΔ3TOK1Δ cells transformed with pYES2-NcTOKA and pYES2, respectively. (B and C) NcTOKA-mediated inward currents. The pipette solution included the following: 100 mM KCl, 5 mM $MgCl_2$, 3 mM K_2ATP, 10 mM HEPES, 4 mM EGTA, and 20 mM KOH (pH 7.4). (B) Whole-cell currents recorded by using SBS containing 60 mM KCl and 1 mM $CaCl_2$ resulting from voltage steps to 20, −20, and −100 mV from a holding potential of −80 mV. Note that the E_K was −16 mV. (C) Current-voltage relationship of NcTOKA currents from the same cells shown in panel A. Solid and dashed lines represent data from cells in SBS containing 10 and 60 mM K^+, respectively. (D) Typical current-voltage relationship of NcTOKA whole-cell currents recorded by using SBS containing 1 (▲), 10 (■), and 60 (▼) mM KCl. Calculated K^+ equilibrium potentials (E_{rev}) for each solution are indicated by arrows below the *x* axis. (Inset) Relationship between steady-state chord conductance NcTOKA currents and voltage. Chord conductance (G) was calculated as $I_{ss}/(V_m - E_K)$, where I_{ss} is the steady-state current at test voltage (V_m). Data were fitted (by using Clampfit 8.1) to a Boltzman equation of the form $G = G_{max}/[1 + \exp(V_m - V_{0.5})/S]$, where G is the chord conductance at test voltage (V_m), G_{max} is the maximal chord conductance, $V_{0.5}$ is the voltage at which G is half maximal, and S is the slope factor equivalent to $RT/\delta F$, where δ is the apparent gating charge and R, T, and F have their usual meanings. For data presented at 1 mM K^+, G_{max} = 12.1 nS and $V_{0.5} = -29$ mV; at 10 mM K^+, G_{max} = 15.8 nS and $V_{0.5} = -5.2$ mV; and at 60 mM K^+, G_{max} = 13.1 nS and $V_{0.5} = +32$ mV. The δ value for all fittings was 1.2.

K^+, the voltage at which half-maximal conductance occurred ($V_{0.5}$) was −36 ± 3.2 mV (n = 5), −3.9 ± 2.9 mV (n = 6), and +39 mV (n = 2), respectively, indicating that NcTOKA gating was sensitive to extracellular K^+. Note that at concentrations of >10 mM extracellular K^+, the $V_{0.5}$ followed exactly the changes in E_K (i.e., increasing the K^+ concentration from 10 to 60 mM resulted in $V_{0.5}$ and E_K shifts of −42.9 and −43 mV, respectively). However, reducing the extracellular K^+ to 1 mM resulted in a shift of $V_{0.5}$ of 32.1 mV for a 10-fold change in K^+, indicating a reduced sensitivity of NcTOKA gating to K^+ at low extracellular K^+ concentrations. A similar phenomenon has also been observed for ScTOK1 currents (37) which has been suggested to reflect a binding site with moderate affinity (>1 mM) for extracellular K^+, which is responsible for the sensitivity of the gating process to extracellular K^+.

Single-channel recordings. Single-channel activity such as that shown in Fig. 6 was observed in outside-out patches from three independent yeast cells expressing NcTOKA. The E_{rev} and unitary conductance of the channel were −50 mV and 16 pS, respectively, in SBS containing 10 mM KCl and 10 mM $CaCl_2$. This is similar to those recorded for ScTOK1, with both NcTOKA and ScTOK1 displaying rapid flickering between the open and closed states (4). In addition, averaging single-channel current recordings showed that the channels had similar time dependence of activation to that observed for the whole-cell current (compare Fig. 3A and 6C). These results indicate that Fig. 6A represents NcTOKA channel activity. It is noteworthy that the single-channel current of NcTOKA was ca. 1 pA at +44 mV. Using the same recording conditions, the average whole-cell current from NcTOKA-expressing cells was ~300 pA (Fig. 1D), indicating that ca. 300 channels were expressed per cell. Taking the average cell diameter to be 4 μm (see Materials and Methods), this indicated that the GAL1

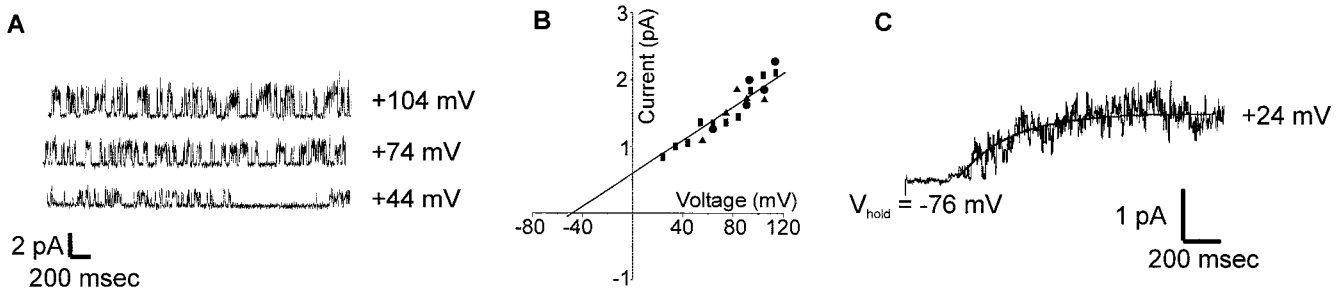

FIG. 6. Properties of NcTOKA single-channel currents. The bath solution was SBS containing 10 mM KCl and 10 mM $CaCl_2$. (A) Recordings from an outside patch. The holding voltages from each recording are shown on the right. Upward deflections represent channel openings. (B) Single-channel current as a function of voltage. Different symbols represent recordings from different patches. The unitary conductance (*G*) and reversal potential (E_{rev}) were determined by fitting a linear regression to the data. *G* was 16 pS and E_{rev} was −50 mV. (C) Least-squares fit of equation 1 (see Fig. 3) to data from 30 separate current recordings from an isolated patch in which the voltage was stepped from −76 mV to + 24 mV. The τ value was 285 ms.

promoter (which is a relatively strong promoter) was able to express to a density of 6 channels per μm^{-2}.

Pharmacology. The pharmacology of NcTOKA was studied in whole-cell patch clamp conditions by using SBS containing 10 mM KCl. Currents were blocked by extracellular Ca^{2+} (Fig. 7); the block was voltage independent and fully reversible (data not shown). Typically, up to 90% of the NcTOKA current was inhibited by increasing Ca^{2+} from 0.1 to 40 mM (corresponding Ca^{2+} activities: 57 μM to 13 mM) with a K_i of 2.7 mM (Ca^{2+} activity). Voltage-independent, dose-dependent blocks of NcTOKA currents were also observed with extracellular application of verapamil (200 μM reduced currents by 75%), TEA+ (20 mM reduced currents by ca. 50%), and quinine (5 mM reduced currents by ca. 60%). Known blockers of other K^+ channels, such as Cs^+ (up to 10 mM), 4-aminopyridine (up to 100 μM), and glibenclamide (up to 50 μM), had no effect on NcTOKA currents.

DISCUSSION

The present study is the first to clone and electrophysiologically characterize an ion channel from a filamentous fungus. The difficulty in applying the PCT to filamentous fungi (see the introduction) has resulted in a relative dearth of knowledge regarding the electrophysiological properties of ion channels in fungi and their role in hyphal growth. Although the laser-assisted PCT allowed the first detailed recordings of ion channels in fungal hyphal cells (30), this technique has resulted in only one other publication (38). Therefore, the ability to clone and functionally express *Neurospora* ion channels in yeast cells provides an alternative (and possibly a more amenable) approach to the electrophysiological study of ion transporters in filamentous fungi, which should significantly aid the investigation of ion channel function in fungal physiology.

The hydropathy profile of NcTOKA indicated that it belonged to the relatively new two pore domain family of K^+ channels (10) with an overall structural motif identifying it as a TOK1 homolog. The K^+ signature motif of TXGYGD, which is associated with ion selectivity of K^+ channels, is well conserved in both P domains of NcTOKA (Fig. 1C, residues 14 to 19). It is noteworthy that the TXGYGD motif is perfectly conserved in NcTOKA P2, whereas in NcTOKA P1 Tyr-17 is replaced with a Phe residue. A similar arrangement was observed for ScTOK1 P2 in which Tyr-17 is replaced by a Leu residue (18). The significance of the Phe residue in NcTOKA P2 on the selectivity of NcTOKA is not known, but site-directed mutagenesis indicated that the Leu residue in P2 of ScTOK1 was essential for channel function (18).

The outward whole-cell currents recorded in NcTOKA-expressing *WΔ3TOK1Δ* yeast cells could be unequivocally attributed to NcTOKA activation by the following observations. First, the outward currents were galactose inducible; this is consistent with the switching of the GAL1 promoter, and its controlled NcTOKA expression, on or off with galactose or glucose, respectively. Second, the three genes known to encode for K^+ transporters (i.e., TRK1, TRK2, and TOK1) have been "knocked out" in *WΔ3TOK1Δ* cells and, as a consequence, they exhibit no endogenous currents in the patch clamp conditions used in the present study. Thus, the absence of any interference from endogenous currents makes the yeast system particularly suited for the analysis of heterologously expressed K^+ transporters. Note that in extracellular solutions containing low divalent cation concentrations (i.e., <0.1 mM), yeast cells exhibit a time-dependent inward current at negative potentials (5, 31). However, in the present study, most of the extracellular solutions contained at least 1 mM Ca^{2+}, which is sufficient to block any interference from this endogenous current.

Comparison with ScTOK1-mediated currents. NcTOKA whole-cell currents exhibited several electrophysiological properties similar to that reported for ScTOK1. NcTOKA exhibited time-dependent and instantaneously activating currents, the magnitude of each being dependent on the holding potential. That is, activation from more negative holding potentials reduced the contribution of the instantaneous component. As has been reported for ScTOK1, the NcTOKA-mediated time-dependent component activated with approximately mono-exponential kinetics (18, 37). These properties have led ScTOK1 to be modeled as a C1 ↔ C2 ↔ O transition (18), where C2 represents the channel occupying a shallow state which proceeds to the open state very rapidly (instantaneously) and C1 represents the channel occupying a deeper closed state. Activation from this state gives rise to a time-dependent component reflecting the slower transition to the open state via the C2 closed state. The data in the present study are consistent

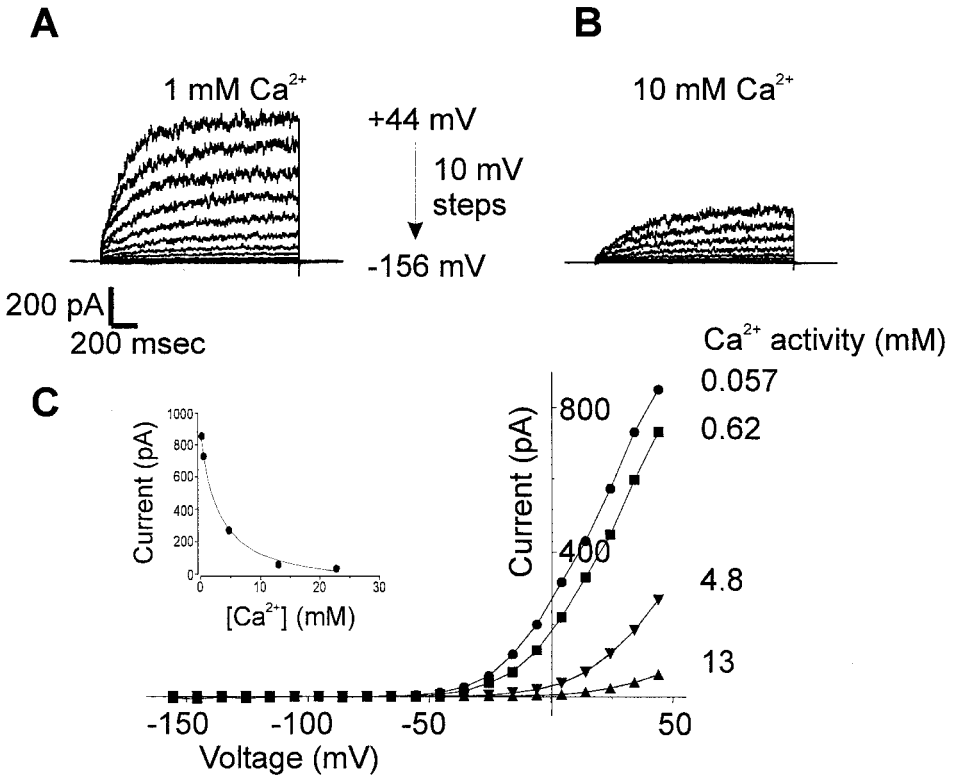

FIG. 7. Effect of increasing extracellular Ca^{2+} on NcTOKA currents. SBS containing 10 mM KCl and various concentrations of $CaCl_2$ was used. The holding potential was −76 mV, and voltage pulses ranged from +44 to −156 mV in 10-mV steps. (A and B) The extracellular Ca^{2+} concentration was varied between 0.1 and 40 mM, but only currents in 1 (A) and 10 (B) mM are shown. (C) Current-voltage relationship of NcTOKA currents with various extracellular Ca^{2+} activities. (Inset) Inhibition of currents at +44 mV plotted as a function of extracellular Ca^{2+} activity. Data were fitted with equation 2: $I_{obs} = I_{max} - [(I_{min}\,[Ca])/(K_i + Ca)]$ where I_{max} is current in the absence of Ca^{2+} (961 pA), I_{min} is the current at saturating Ca^{2+} (78 pA), [Ca] is the extracellular Ca^{2+} activity, and K_i is the inhibition constant for Ca^{2+} (activity of 2.8 mM).

with this three-state model. It is noteworthy that tail currents have not been reported for ScTOK1, suggesting that the transition from the open to the closed state is very rapid (or instantaneous). In contrast, small time-dependent NcTOKA-mediated tail currents could be measured (see Fig. 4 and 5B), which suggests that the transition from the open to the closed state for NcTOKA is relatively slower than that for ScTOK1. However, there have been no studies that have focused on identifying ScTOK1-mediated tail currents, and it is possible that small tail currents have been overlooked.

More recently, random mutagenesis identified a "postpore region" (PP region) in the carboxyl-terminal region of the channel occupying the ends of the S6 and S8 TMS domains (25). Mutations in this region (specifically T322I, V456I, and S330F) dramatically affected the activation of ScTOK1 from the C1 state such that PP region-mutated channels more readily resided in the C2 state and lacked the delayed, time-dependent activation from the C1 state. Thus, the PP region was identified as playing an important role in ScTOK1 gating, specifically in the stability of the C1 state. More recently, the involvement of the carboxyl terminus in ScTOK1 gating has been further confirmed by experiments in which the majority of the C terminus is deleted and the "tailless" channels display increased deactivation rates (22, 23). However, a comparison of the C-terminus region of the NcTOKA channel with that of ScTOK1 (including the equivalent region representing the PP region) failed to identify comprehensive conservation of primary amino acid sequences. Specifically, the amino acid residues identified to be important in the regulation of gating in the PP region were not conserved in NcTOKA (data not shown).

Activation of NcTOKA and activation of ScTOK1 are both dependent on extracellular K^+ such that the activation potential is dependent on the driving force for K^+ ($V_m - E_K$). This is the same as that described for K^+-selective inwardly rectifying channels in animal cells (16). However, rectification of the inward currents in animal cells results from the chronic obstruction by internal Mg^{2+} or polyamines, whereas ScTOK1 rectification has been reported to be cation independent and is thought to result from an intrinsic property of the channel (18, 24). The attributes of rectification were not investigated for NcTOKA currents, though no differences in the rectification of the outward currents were observed upon removal of the Mg^{2+} from the extracellular solution in the present study (data not shown). Furthermore, both ScTOK1 and NcTOKA mediate small inward K^+ currents, and their expression is capable of overcoming the K^+-limiting growth phenotype of *trk1*Δ *trk2*Δ cells (7).

A distinguishing feature of NcTOKA currents was that they were inhibited by extracellular Ca^{2+} (with up to 90% inhibition

with 20 mM Ca^{2+}). This is consistent with NcTOKA possessing a binding site with moderate affinity for extracellular Ca^{2+}, which when occupied is capable of inhibiting K^+ permeation. This is in contrast to ScTOK1. Although no systematic study of extracellular Ca^{2+} inhibition of ScTOK1 has been reported, Roberts et al. (31) and Bihler et al. (5) have shown that no significant inhibition of ScTOK1-mediated outward currents is apparent upon increasing extracellular the Ca^{2+} concentration from 0.1 to 10 mM.

Physiological significance. The plasma membrane of *Neurospora* is normally hyperpolarized to potentials negative of E_K (see, for example, references 32 and 34). The present study illustrates that NcTOKA mediates K^+ influx at a potential negative of E_K and, consistent with this, is able to rescue the K^+-limiting growth phenotype of a yeast mutant defective in K^+ uptake. Thus, it is possible that NcTOKA mediates K^+ uptake in *N. crassa* under most conditions.

It is well documented that K^+-starved *Neurospora* exhibits high- and low-affinity transport exhibiting K_m values of ca. 20 μM and 10 mM, respectively (29). This is analogous to the dual-uptake mechanism found in plant roots (6). High-affinity K^+ uptake in *Neurospora* is via a H^+-K^+ symporter, identified recently as a HAK1 homologue (15). However, even in media containing as little as 50 μM K^+, Rodriguez-Navarro et al. (33) showed that, under some conditions, the membrane potential of *Neurospora* was sufficiently negative (up to −300 mV) to allow passive "channel-mediated" K^+ uptake; thus, NcTOKA could contribute to K^+ uptake even in conditions of low extracellular K^+. Indeed, the advantage of K^+ uptake via NcTOKA is that it is energetically less expensive to acquire K^+ passively than via H^+/K^+ symport activity. Furthermore, K^+ uptake via the H^+-K^+ symporter is pH dependent, with peak activity at approximately pH 6.0 and significantly reduced activity under more acidic and more alkaline conditions. In addition, the high-affinity K^+ uptake mechanism is repressed in *Neurospora* grown in K^+-replete conditions. Thus, channel-mediated K^+ uptake in *Neurospora* may be important in suboptimal conditions for symporter activity. The identity of the low-affinity pathway(s) in *Neurospora* is unknown, although clearly K^+ uptake via NcTOKA could contribute to this.

Under conditions that induce plasma membrane depolarization in *Neurospora* to potentials positive of E_K, NcTOKA would mediate K^+ efflux, for example, by reducing extracellular pH to <4 (33) (Table 3). Under these conditions, NcTOKA activation could play a role in membrane potential stabilization and prevent deleterious depolarization of the membrane. Furthermore, *Neurospora* plasma membrane potential has been shown to oscillate, which can result in membrane potential depolarizations to values positive of E_K (35). Although the physiological relevance of these oscillations is unclear, NcTOKA could play a role in the propagation of the oscillation, similar to the role of K^+ channels in the propagation of an action potential in "excitable" cells. It should also be noted that the activation of NcTOKA may be modulated by cytosolic second messengers that could result in channel activation over a wider range of physiological conditions. Indeed, it is a characteristic feature of two-P-domain K^+ channels that their activation is modulated by a wide array of stimuli and messengers (e.g., cytosolic pH, phosphorylation and/or dephosphorylation, and mechanostress [19]). The regulation of NcTOKA by second messengers can be relatively easily addressed by using the PCT and varying the composition of the pipette medium.

In conclusion, K^+ channels are likely to be present in the plasma membrane of all organisms, and thus it can be concluded that the regulation of K^+ fluxes across the membrane is essential for the survival of all organisms. The identification and characterization of the TOK1 homolog in the present study represent a first step in identifying the role of K^+ channels and the importance of controlling K^+ fluxes across the plasma membrane in filamentous fungi.

ACKNOWLEDGMENTS

I thank Delphine Oddon for technical assistance and Eugene Diatloff and Julia Davies for comments on the manuscript.

This work was funded by a Research Career Development Fellowship awarded to S.K.R. by the Wellcome Trust.

REFERENCES

1. **Armstrong, C. M., and B. Hille.** 1998. Voltage-gated ion channels and electrical excitability. Neuron **20:**371–380.
2. **Assmann, S. M., and L. L. Haubrick.** 1996. Transport proteins of the plant plasma membrane. Curr. Opin. Cell Biol. **8:**458–467.
3. **Bertl, A., and C. L. Slayman.** 1992. Complex modulation of cation channels in the tonoplast and plasma membrane of *Saccharomyces cerevisiae*: single-channel studies. J. Exp. Biol. **172:**271–287.
4. **Bertl, A., H. Bihler, C. Kettner, and C. L. Slayman.** 1998. Electrophysiology in the eukaryotic model cell *Saccharomyces cerevisiae*. Pflugers Arch. Eur. J. Physiol. **436:**999–1013.
5. **Bihler, H., C. L. Slayman, and A. Bertl.** 1998. NSC1: a novel high-current inward rectifier for cations in the plasma membrane of *Saccharomyces cerevisiae*. FEBS Lett. **432:**59–64.
6. **Epstein, E., D. W. Rains, and O. E. Elzam.** 1963. Resolution of dual mechanisms of potassium absorption by barley roots. Proc. Natl. Acad. Sci. USA **49:**684–692.
7. **Fairman, C., X. L. Zhou, and C. Kung.** 1999. Potassium uptake through the TOK1 K^+ channel in the budding yeast. J. Membr. Biol. **168:**149–157.
8. **Garrill, A., and J. M. Davies.** 1994. Patch clamping fungal membranes: a new perspective on ion transport. Mycol. Res. **98:**257–263.
9. **Gietz, R. D., and R. A. Woods.** 1994. High efficiency transformation in yeast, p. 121–134. *In* J. A. Johnston (ed.), Molecular genetics of yeast: practical approaches. Oxford University Press, Oxford, United Kingdom.
10. **Goldstein, S. A. N., D. Bockenhauer, I. O'Kelly, and N. Zilberberg.** 2001. Potassium leak channels and the KCNK family of two-P-domain subunits. Nat. Rev. Neurosci. **2:**175–184.
11. **Gurr, S. J., S. E. Uncles, and J. R. Kinghorn.** 1987. The structure and organisation of nuclear genes of filamentous fungi, p. 93–139. *In* J. R. Kinghorn (ed.), Gene structure in eucaryotic microbes. IRL Press, London, United Kingdom.
12. **Gustin, M. C., B. Martinac, Y. Saimi, M. R. Culbertson, and C. Kung.** 1986. Ion channels in yeast. Science **233:**1195–1197.
13. **Gustin, M. C., X. L. Zhou, B. Martinac, and C. Kung.** 1988. A mechanosensitive ion channel in the yeast plasma membrane. Science **242:**762–765.
14. **Hamill, O. P., A. Marty, E. Neher, B. Sakmann, and F. J. Sigworth.** 1981. Improved patch clamp techniques for high resolution current recording from cells and cell-free membrane patches. Pfluegers Arch. **391:**85–100.
15. **Haro, R., L. Sainz, F. Rubio, and A. Rodriguez-Navarro.** 1999. Cloning of two genes encoding potassium transporters in *Neurospora crassa* and expression of corresponding cDNAs in *Saccharomyces cerevisiae.* Mol. Microbiol. **31:**511–520.
16. **Hille, B.** 1992. Ionic channels of excitable membranes. Sinauer Associates, Inc., Sunderland, Mass.
17. **Ketchum, K. A., W. J. Joiner, A. J. Sellers, L. K. Kaczmarek, and S. A. N. Goldstein.** 1995. A new family of outwardly rectifying potassium channel proteins with 2 pore domains in tandem. Nature **376:**690–695.

17a. **Kyte, J., and R. F. Doolittle.** 1982. A simple method for displaying the hydropathic character of a protein. J. Mol. Biol. **157:**105–132.

18. **Lesage, F., E. Guillemare, M. Fink, F. Duprat, M. Lazdunski, G. Romey, and J. Barhanin.** 1996. A pH-sensitive yeast outward rectifier K^+ channel with two pore domains and novel gating properties. J. Biol. Chem. **271:**4183–4187.
19. **Lesage, F., and M. Lazdunski.** 2000. Molecular and functional properties of two-pore-domain potassium channels. Am. J. Physiol. Renal Physiol. **279:** F793–F801.
20. **Levina, N. N., R. R. Lew, G. J. Hyde, and I. B. Heath.** 1995. The roles of Ca^{2+} and plasma membrane ion channels in hyphal tip growth of *Neurospora crassa*. J. Cell Sci. **108:**3405–3417.
21. **Lew, R. R.** 1998. Mapping fungal ion channel locations. Fungal Genet. Biol. **24**:69–76.

22. **Loukin, S. H., J. Y. Lin, U. Athar, C. Palmer, and Y. Saimi.** 2002. The carboxyl tail forms a discrete functional domain that blocks closure of the yeast K^+ channel Proc. Natl. Acad. Sci. USA **99:**1926–1930.
23. **Loukin, S. H., and Y. Saimi.** 2002. Carboxyl tail prevents yeast K^+ channel closure: proposal of an integrated model of TOK1 gating. Biophys. J. **82:** 781–792.
24. **Loukin, S. H., and Y. Saimi.** 1999. K^+-dependent composite gating of the yeast K^+ channel, Tok1. Biophys. J. **77:**3060–3070.
25. **Loukin, S. H., B. Vaillant, X. L. Zhou, E. P. Spalding, C. Kung, and Y. Saimi.** 1997. Random mutagenesis reveals a region important for gating of the yeast K^+ channel YKC1. EMBO J. **16:**4817–4825.
26. **Neher, E.** 1992. Correction for liquid junction potentials in patch clamp experiments. Methods Enzymol. **207:**123–131.
27. **Palmer, C. P., X. L. Zhou, J. Y. Lin, S. H. Loukin, C. Kung, and Y. Saimi.** 2001. A TRP homolog in *Saccharomyces cerevisiae* forms an intracellular Ca^{2+}-permeable channel in the yeast vacuolar membrane. Proc. Natl. Acad. Sci. USA **98:**7801–7805.
28. **Parker, D. R., W. A. Norvell, and R. L. Chaney.** 1995. GEOCHEM-PC: a chemical speciation program for IBM and compatible computers, p. 253–269. *In* R. H. Loeppert, A. P. Schwab, and S. Goldberg (ed.), Chemical equilibrium and reaction models. Special publication 42. Soil Science Society of America, Madison, Wis.
29. **Ramos, J., and A. Rodriguez-Navarro.** 1985. Rubidium transport in *Neurospora crassa.* Biochim. Biophys. Acta **815:**97–101.
30. **Roberts, S. K., G. K. Dixon, S. J. Dunbar, and D. Sanders.** 1997. Laser ablation of the cell wall and localized patch clamping of the plasma membrane in the filamentous fungus *Aspergillus*: characterization of an anion-selective efflux channel. New Phytol. **137:**579–585.
31. **Roberts, S. K., M. Fischer, G. K. Dixon, and D. Sanders.** 1999. Divalent cation block of inward currents and low-afinity K^+ uptake in *Saccharomyces cerevisiae.* J. Bacteriol. **181:**291–297.
32. **Rodriguez-Navarro, A., M. R. Blatt, and C. L. Slayman.** 1986. A potassium-proton symport in *Neurospora crassa.* J. Gen. Physiol. **87:**649–674.
33. **Rodriguez-Navarro, A., and J. Ramos.** 1986. Two systems mediate rubidium uptake in *Neurospora crassa*: one exhibits the dual-uptake isotherm. Biochim. Biophys. Acta **857:**229–237.
34. **Silverman-Gavrila, L. B., and R. R. Lew.** 2000. Calcium and tip growth in *Neurospora crassa.* Protoplasma **213:**203–217.
35. **Slayman, C. L., W. S. Scott, and D. Gradmann.** 1976. "Action potentials" in *Neurospora crassa*, a mycelial fungus. Biochim. Biophys. Acta **426:**732–744.
36. **Taylor, A. R., and C. Brownlee.** 1992. Localized patch clamping of plasma membrane of a polarized plant cell: laser microsurgery of the *Fucus spiralis* rhizoid cell-wall. Plant Physiol. **99:**1686–1688.
37. **Vergani, P., T. Miosga, S. M. Jarvis, and M. R. Blatt.** 1997. Extracellular K^+ and Ba^{2+} mediate voltage-dependent inactivation of the outward-rectifying K^+ channel encoded by the yeast gene TOK1. FEBS Lett. **405:**337–344.
38. **Véry, A. A., and J. M. Davies.** 1998. Laser microsurgery permits fungal plasma membrane single ion channel resolution at the hyphal tip. Applied Environ. Microbiol. **64:**1569–1572.
39. **Watts, H. J., A. A. Véry, T. H. S. Perera, J. M. Davies, and N. A. R. Gow.** 1998. Thigmotropism and stretch-activated channels in the pathogenic fungus *Candida albicans.* Microbiology **144:**689–695.
40. **Zhou, X. L., M. A. Stumpf, H. C. Hoch, and C. Kung.** 1991. A mechanosensitive channel in whole cells and in membrane patches of the fungus *Uromyces*. Science **253:**1415–1417.
41. **Zhou, X. L., B. Vaillant, S. H. Loukin, C. Kung, and Y. Saimi.** 1995. YKC1 encodes the depolarization-activated K^+ channel in the plasma membrane of yeast. FEBS Lett. **373:**170–176.